MIT Libraries | DSpace@MIT

MIT Open Access Articles

Submillimetre galaxies in cosmological hydrodynamical simulations – an opportunity for constraining feedback models

The MIT Faculty has made this article openly available. ***Please share*** how this access benefits you. Your story matters.

Citation: Hayward, Christopher C, Sparre, Martin, Chapman, Scott C, Hernquist, Lars, Nelson, Dylan et al. 2021. "Submillimetre galaxies in cosmological hydrodynamical simulations – an opportunity for constraining feedback models." Monthly Notices of the Royal Astronomical Society, 502 (2).

As Published: 10.1093/MNRAS/STAB246

Publisher: Oxford University Press (OUP)

Persistent URL: https://hdl.handle.net/1721.1/142389

Version: Author's final manuscript: final author's manuscript post peer review, without publisher's formatting or copy editing

Terms of use: Attribution-NonCommercial-ShareAlike 4.0 International

Massachusetts Institute of Technology

Submillimetre galaxies in cosmological hydrodynamical simulations – an opportunity for constraining feedback models

Christopher C. Hayward[1★], Martin Sparre[2,3,4], Scott C. Chapman[5], Lars Hernquist[6], Dylan Nelson[7], Rüdiger Pakmor[7], Annalisa Pillepich[8], Volker Springel[7], Paul Torrey[9], Mark Vogelsberger[4], and Rainer Weinberger[6]

[1]*Center for Computational Astrophysics, Flatiron Institute, 162 Fifth Avenue, New York, NY 10010, USA*
[2]*Institut für Physik und Astronomie, Universität Potsdam, Karl-Liebknecht-Str. 24/25, 14476 Golm, Germany*
[3]*Leibniz-Institut für Astrophysik Potsdam (AIP), An der Sternwarte 16, 14482 Potsdam, Germany*
[4]*Department of Physics, Kavli Institute for Astrophysics and Space Research, Massachusetts Institute of Technology, Cambridge, MA 02139, USA*
[5]*Department of Physics and Atmospheric Science, Dalhousie University, 6310 Coburg Road, Halifax B3H 4R2, Canada*
[6]*Harvard-Smithsonian Center for Astrophysics, 60 Garden Street, Cambridge, MA 02138, USA*
[7]*Max-Planck-Institut für Astrophysik, Karl-Schwarzschild-Str. 1, D-85741 Garching, Germany*
[8]*Max-Planck-Institut für Astronomie, Königstuhl 17, D-69117, Heidelberg, Germany*
[9]*Department of Astronomy, University of Florida, 211 Bryant Space Sciences Center, Gainesville, FL 32611, USA*

11th February 2021

arXiv:2007.01885v3 [astro-ph.GA] 10 Feb 2021

ABSTRACT

Submillimetre galaxies (SMGs) have long posed a challenge for theorists, and self-consistently reproducing the properties of the SMG population in a large-volume cosmological hydrodynamical simulation has not yet been achieved. We use a scaling relation derived from previous simulations plus radiative transfer calculations to predict the submm flux densities of simulated SMGs drawn from cosmological simulations from the *Illustris* and *IllustrisTNG* projects based on the simulated galaxies' star formation rates (SFRs) and dust masses and compare the predicted number counts with observations. We find that the predicted SMG number counts based on *IllustrisTNG* are significantly less than observed (more than 1 dex at $S_{850} \gtrsim 4$ mJy). The simulation from the original *Illustris* project yields more SMGs than *IllustrisTNG*: the predicted counts are consistent with those observed at both $S_{850} \lesssim 5$ mJy and $S_{850} \gtrsim 9$ mJy and only a factor of ~ 2 lower than observed at intermediate flux densities. The redshift distribution of SMGs with $S_{850} > 3$ mJy in *IllustrisTNG* is consistent with the observed distribution, whereas the *Illustris* redshift distribution peaks at significantly lower redshift (1.5 vs. 2.8). We demonstrate that *IllustrisTNG* hosts fewer SMGs than *Illustris* because in the former, high-mass ($M_\star \sim 10^{11}$ M$_\odot$) $z \sim 2-3$ galaxies have lower dust masses and SFRs than in *Illustris* owing to differences in the sub-grid models for stellar or/and active galactic nucleus (AGN) feedback between the two simulations (we unfortunately cannot isolate the specific cause(s) post hoc). Our results demonstrate that because our method enables predicting SMG number counts in post-processing with a negligible computational expense, SMGs can provide useful constraints for tuning sub-grid models in future large-volume cosmological simulations.

Key words: cosmology: theory – methods: numerical – galaxies: evolution – galaxies: formation – galaxies: star formation – galaxies: starburst.

1 INTRODUCTION

Submillimetre galaxies (SMGs) are a class of rapidly star-forming (SFR $\sim 10^2 - 10^3$ M$_\odot$ yr^{-1}), highly dust-obscured galaxies that were discovered in the late 1990s (Smail et al. 1997; Barger et al. 1998; Hughes et al. 1998; Eales et al. 1999; see Casey et al. 2014 for a recent review). Since that time, they have been the focus of much observational work for multiple reasons. For example, they have inferred SFRs that are unprecedented in the local Universe (a 'typical' SMG has an SFR a factor of a few greater than Arp 220, and some have SFRs over an order of magnitude greater). Their SFR surface densities are sufficiently high that they approach the theoretical maximum SFR surface density at which momentum injection from stellar feedback can unbind the remaining gas and thus halt star formation (Scoville 2003; Murray et al. 2005; Thompson et al. 2005). They are estimated to contribute as much as half of the SFR density of the Universe at $z \sim 2-3$ (Chapman et al. 2005; Dunlop et al. 2017; Michałowski et al. 2017; Smith et al. 2017). Their number densities ($N \sim 10^{-5} - 10^{-6}$ cMpc^{-3} at $z \sim 2-3$) and stellar (median $M_\star \sim 10^{11}$ M$_\odot$; e.g. da Cunha et al. 2015; Ma et al. 2015; Miettinen et al. 2017) and halo ($M_\mathrm{h} \sim 10^{13}$ M$_\odot$; Blain et al. 2004; Hickox et al. 2012; Wilkinson et al. 2017) masses suggest that they may be the progenitors of compact quiescent galaxies (Toft et al. 2014). SMGs at $z \gtrsim 3$ serve as beacons of the highest-mass dark matter halos at a given epoch (Miller et al. 2015, 2020), potentially enabling tests of ΛCDM (Marrone et al. 2018). Most importantly for the present

★ E-mail: chayward@flatironinstitute.org

© 2020 The Authors

work, reproducing the observed SMG number counts and redshift distribution has posed a challenge for theorists since their discovery (Baugh et al. 2005; Primack 2012), and their physical nature is still vigorously debated.

Modelling the SMG population self-consistently is extremely challenging. Because of their rarity, large volumes must be simulated. However, one must also resolve individual galaxies sufficiently well to capture physical processes that may be responsible for their high SFRs, including the classical explanation, merger-induced starbursts (e.g. Engel et al. 2010; Chakrabarti et al. 2008; Narayanan et al. 2010; Hayward et al. 2011), and disc instabilities (Lacey et al. 2016). Moreover, to accurately model SMGs, one must predict submm fluxes of simulated galaxies because there is not a one-to-one relation between submm flux density and SFR, mainly owing to the dependence of the dust temperature distribution and thus submm flux density on the dust mass in addition to the SFR (Hayward et al. 2011; Safarzadeh et al. 2016). For this purpose, it is necessary to perform dust radiative transfer, the results of which depend on the distribution of dust and sources of emission (stars and active galactic nuclei, AGN) on sub-galactic scales.

For the above reasons, hybrid approaches – rather than large-volume cosmological simulations with full radiative transfer – have typically been employed to model the SMG population. The earliest theoretical studies about SMGs employed semi-analytic models, in which submm fluxes were predicted via simplified radiative transfer calculations assuming an idealised axisymmetric geometry (e.g. Granato et al. 2000; Baugh et al. 2005) or using an analytic model for dust attenuation and empirical SED templates (e.g. Somerville et al. 2012). Granato et al. (2000) compared the SMG number counts and redshift distribution predicted by the GALFORM (Cole et al. 2000) SAM with that observed. They found that the model under-predicted the observed counts by a factor of $\sim 20-30$. Other SAMs (Fontanot et al. 2007; Somerville et al. 2012) also significantly under-predicted the bright SMG number counts. Baugh et al. (2005) explored various modifications to the GALFORM model, searching for a means to match the SMG number counts and redshift distribution while not violating other observational constraints, such as the $z = 0$ stellar mass function. They found that by assuming a flat stellar initial mass function (IMF) in starbursts (specifically, $dn/d\log m$ = constant for the mass range $0.15 < m/\mathrm{M}_\odot < 125$), in addition to other subdominant modifications to the model, they were able to reproduce the SMG number counts and redshift distribution. In the Baugh et al. (2005) model, SMGs are predominantly minor merger-driven starbursts (González et al. 2011). However, due to the many free parameters employed in SAMs, it is possible to find multiple qualitatively distinct solutions that satisfy observational constraints equally well (e.g. Lu et al. 2011; Henriques et al. 2013), so it is unclear that a top-heavy IMF is necessary, rather than simply sufficient given the other components of the model, to reproduce the SMG population. Indeed, in the current version of the GALFORM model (Lacey et al. 2016), the IMF assumed for starbursts, $dn/d\log m \propto m^{-1}$, is still top-heavy compared to the Kroupa (2001) IMF ($dn/d\log m \propto m^{-1.3}$ for $m > 0.5\ \mathrm{M}_\odot$) but considerably steeper than that assumed by Baugh et al. (2005), and SMGs are predominantly starbursts driven by disc instabilities rather than mergers (Cowley et al. 2015; Lacey et al. 2016). Moreover, Safarzadeh et al. (2017) demonstrated that the SMG number counts and redshift distribution predicted based on the Lu et al. (2014) SAM, which uses a standard Chabrier (2003) IMF, agree reasonably well with observations.

Some studies have employed approaches based on performing post-processing dust radiative transfer on idealised (non-cosmological) galaxy merger simulations. Narayanan et al. (2010, see also Chakrabarti et al. 2008; Hayward et al. 2011, 2012) demonstrated that merger-induced starbursts could produce submm flux densities as high as observed. Hayward et al. (2013a) combined the results of isolated disc and galaxy merger simulations with a semi-empirical model for the redshift evolution of galaxy mass functions, merger rates, gas fractions and other properties to predict the SMG number counts and redshift distribution, finding good agreement with observations despite employing a standard Kroupa (2001) IMF. In their model, SMGs are a mix of isolated 'quiescently' star-forming disc galaxies, pre-coalescence mergers blended into a single submm source (see below), and merger coalescence-induced starbursts. Although the hybrid approach employed by Hayward et al. (2013a) satisfies various observational constraints, such as the $z = 0$ stellar mass function, by construction, one significant downside is that it effectively sidesteps some important issues, such as self-consistently predicting the correct $z \sim 2-3$ stellar mass function, and is far from 'ab initio'.

Narayanan et al. (2015) performed radiative transfer in post-processing on a zoom simulation of a halo with a $z = 2$ halo mass of $3 \times 10^{13}\ \mathrm{M}_\odot$. The central galaxy reached a peak submm flux density of $S_{850} \sim 25$ mJy, comparable to the flux densities of the brightest SMGs known (Hayward 2013). Narayanan et al. (2015) argued that major mergers did not play an important role in driving the galaxy's high submm flux density. They posited that SMGs are typically massive galaxies undergoing minor mergers and that stellar feedback – which results in bursts of star formation, subsequent outflows, and re-accretion in a 'galactic fountain' (Muratov et al. 2015; Sparre et al. 2017; Hayward & Hopkins 2017) – 'saves' gas accreted by the halo for consumption at $z \sim 2-3$, thus resulting in an SMG phase consistent with the peak of the observed SMG redshift distribution. However, as with idealised, non-cosmological simulations, zoom simulations suffer from a lack of statistics; thus, Narayanan et al. (2015) did not present predictions for the SMG number counts and redshift distribution, and it may not be possible to infer the nature of a 'typical' SMG from the evolution of a single halo.

Despite the aforementioned difficulties in using large-volume cosmological hydrodynamical simulations to model the SMG population, there have been a few such works published to date. Davé et al. (2010) performed a hydrodynamical simulation with a volume of $(96h^{-1}\ \mathrm{Mpc})^3$. Given an estimate for the number density of $z \sim 2$ SMGs ($1.5 \times 10^{-5}\ \mathrm{cMpc}^{-3}$), they computed the expected number of SMGs that the simulation should contain, 41, and analysed the 41 most rapidly star-forming galaxies in the $z = 2$ snapshot (effectively assuming a monotonically increasing relationship between submm flux density and SFR). In the Davé et al. (2010) model, SMGs correspond to the high-mass ($M_\star \sim 10^{11-11.7}\ \mathrm{M}_\odot$) end of the star-forming galaxy 'main sequence', and their star formation is typically not driven by major mergers. The properties of the simulated galaxies agreed well with some of the observed properties of SMGs, but the SFRs were lower than those inferred for real SMGs by a factor of ~ 3. Davé et al. (2010) noted that one possible explanation for this discrepancy is that the observationally inferred SFRs, which rely on the assumption of a standard Milky Way-type IMF, would overestimate the true SFR of SMGs if the IMF in SMGs were top-heavy, as argued in some of the works mentioned above. However, we note that at $z = 2$, at fixed stellar mass, *all* galaxies in the Davé et al. (2010) simulation, not only the SMG analogues, have SFRs lower than observed (i.e. the normalisation of the $z \sim 2$ SFR–stellar mass relation in the simulation is systematically below that observed). Consequently, reconciling the SFRs of the observed and simulated galaxies would require a top-heavy IMF in lower-mass, more-typical galaxies in addition to SMGs.

Shimizu, Yoshida & Okamoto (2012) performed a cosmological hydrodynamical simulation with a comoving volume of $(100h^{-1}\,\mathrm{Mpc})^3$. They employed a simple model to predict the submm flux densities of their simulated galaxies: assuming a spherically symmetric dust geometry, they computed the total luminosity absorbed by dust. Then, assuming dust of a single temperature in thermal equilibrium and neglecting dust self-absorption, they computed the submm flux densities of their simulated galaxies. Their predicted counts agree well with those observed for $S_{850} \gtrsim 1$ mJy, but they under-predict the counts of fainter sources. However, this success should be taken with a grain of salt, as their simplified model for computing the submm flux density may over-predict the submm flux density: applying the same model (i.e. using the $S_{850}(\mathrm{SFR}, M_{\mathrm{dust}})$ scaling for an optically thin single-temperature modified blackbody) to hydrodynamical simulations of isolated disc galaxies and galaxy mergers on which they performed radiative transfer, Hayward et al. (2011) found that the simplified model over-predicts the flux densities (relative to the results of the radiative transfer calculations) by $\sim 0.3-0.5$ dex. Because of the steepness of the bright end of the SMG number counts, reducing the predicted fluxes of their model SMGs by this seemingly modest factor would cause the number counts to be significantly under-predicted.

McAlpine et al. (2019) compared the properties of 'submm-bright' galaxies (which they define by $S_{850} \geq 1$ mJy) in the EAGLE simulation (Schaye et al. 2015) with those of observed SMGs. The submm fluxes were computed by performing dust radiative transfer directly on the galaxies from the simulation. Notably, the redshift distribution of sources with $S_{850} \geq 1$ mJy agrees reasonably well with that observed, but the predicted number counts of sources with $S_{850} \geq 3$ mJy are more than two orders of magnitude less than those observed (fig. 9 of Cowley et al. 2019; see also Wang et al. 2019).

Lovell et al. (2020) performed dust radiative transfer on galaxies from SIMBA (Davé et al. 2019). Their predicted counts are closer to those observed than are those for EAGLE or, as we shall see below, *IllustrisTNG*, but they are still a factor of a few to ~ 10 less than observed, and the SMG redshift distribution is skewed toward somewhat higher redshift than observed.

The main advantage of our work (and that of McAlpine et al. 2019 and Lovell et al. 2020) relative to the cosmological-simulation-based SMG studies of Davé et al. (2010) and Shimizu et al. (2012) is how we define SMGs. For this purpose, it is necessary to compute the submm flux density directly because both the SFR and dust mass affect the FIR/submm SED (Hayward et al. 2011; Lanz et al. 2014; Safarzadeh et al. 2016). For this reason, a galaxy with a high SFR but low dust mass may actually have a lower submm flux density than one with a lower SFR but high dust mass, owing to the former galaxy having a 'hotter' SED. Consequently, the monotonic mapping between submm flux density and SFR assumed in Davé et al. (2010) does not hold in detail (Hayward et al. 2011, 2013a). Since the mass and spatial resolution state-of-the-art large-volume cosmological hydrodynamical simulations are possibly still insufficient to perform dust radiative transfer directly on the simulated galaxies (i.e. without resampling in both space and time; Trayford et al. 2017), and to avoid the significant computational expense associated with doing so, we instead assign submm flux densities to our simulated galaxies using a fitting function that gives the submm flux density as a function of SFR and dust mass. The fitting function was derived from the results of performing dust radiative transfer on hydrodynamical simulations of isolated disc and merging galaxies (Hayward et al. 2011, 2013a); see Section 2 for details. As discussed above, this approach is superior to that of Shimizu et al. (2012) because the single-temperature, optically thin modified blackbody scaling assumed in that work tends to over-predict the submm flux densities of the simulated galaxies by a factor of $\sim 0.3-0.5$ dex (Hayward et al. 2011), implying that the SMG number counts presented in Shimizu et al. (2012) are significantly higher than they would be had a more accurate method for computing submm flux densities been used.

One issue that has complicated previous comparisons between theoretical models and observations is blending of multiple SMGs into a single submm source. Models predict that blending of both early-stage mergers (Hayward et al. 2011, 2012, 2013a) and physically unassociated galaxies (Hayward et al. 2013b; Muñoz Arancibia et al. 2015; Cowley et al. 2015) should result in a significant fraction of observed single-dish submm sources breaking up into multiple sources when observed at higher resolution with e.g. ALMA, as has been observed (e.g. Karim et al. 2013; Hodge et al. 2013; Simpson et al. 2015; Hayward et al. 2018). Blending causes the number counts derived from single-dish observations (e.g. those based on SCUBA-2 maps) to exceed the true SMG number counts, as demonstrated explicitly by the comparison of LABOCA and ALMA counts shown in Karim et al. (2013), although the magnitude of this effect is still debated. For simplicity, we do not treat blending of submm sources in this work, so we will compare the simulated SMGs only with ALMA observations of spatially resolved SMGs.

In this work, we show that the SMG number counts predicted from *Illustris* using our simple method are in reasonable agreement with observations, whereas those predicted from *IllustrisTNG* are significantly less than observed. However, it has been shown in numerous previous works that *IllustrisTNG* better reproduces various aspects of the general galaxy population than *Illustris*, and thus the aforementioned result should not be interpreted as an indication that *Illustris* is more correct than *IllustrisTNG*. Instead, our results indicate a need for further revision of the sub-grid models and demonstrate the utility of SMG number counts for constraining said models for future large-volume cosmological simulations, especially given that our method for predicting the SMG counts incurs negligible computational expense.

The remainder of this work is organised as follows: in Section 2, we summarise the *Illustris* and *IllustrisTNG* simulations and the method for generating mock SMG catalogues from these simulations. Section 3 compares the predicted number counts with observations. In Section 4, we outline how our method for predicting SMG number counts from large-volume cosmological simulations can be used to constrain sub-grid feedback models, discuss how the quenched fractions of massive $z \sim 2-3$ galaxies in the simulations compare with observational constraints, and detail some limitations and future work. In Section 5, we conclude.

2 METHODS

2.1 The *Illustris* and *IllustrisTNG* simulations

Here, we summarise the details of the large-volume cosmological simulations from the *Illustris* and *IllustrisTNG* projects used in this work. Both simulations were run using AREPO (Springel 2010), an unstructured moving-mesh hydrodynamics code. The details of the physical model employed in *Illustris* are presented in Vogelsberger et al. (2014a, see also Vogelsberger et al. 2013 and Torrey et al. 2014), so we will only briefly list the key aspects here. The models for star formation and stellar feedback are based on Springel & Hernquist (2003). Star formation is implemented by stochastically spawning stellar particles at a rate set by a volume density-dependent Kennicutt-Schmidt law (Kennicutt 1998; Schmidt 1959); a density

threshold of 0.13 cm^{-3} is employed. An effective equation of state is used to approximate how SNe heat the ISM, and stellar feedback-driven winds are implemented by stochastically kicking and temporarily hydrodynamically decoupling gas cells in a manner intended to capture bipolar winds (Springel & Hernquist 2003). Importantly for the present work, stellar evolution, chemical enrichment, and gas return are tracked. BH accretion is modelled as Eddington-limited modified Bondi-Hoyle accretion with a boost factor to account for the gas density near the BH being underestimated due to resolution, and a two-stage model for AGN feedback, including both quasar and radio modes, is employed (Springel et al. 2005; Sijacki et al. 2007). The sub-grid models were tuned to reproduce the SFR density as a function of redshift and $z = 0$ SFR stellar mass–halo mass and black hole mass–stellar mass relations. Further details about and first results from the *Illustris* simulations are presented in Vogelsberger et al. (2014b,a); Genel et al. (2014); Sijacki et al. (2015). In this work, we use the *Illustris-1* simulation, which has a volume of $(106.5\ \mathrm{Mpc})^3$, 2×1820^3 resolution elements, a dark matter (baryonic) mass resolution of 6.26 $(1.26) \times 10^6\ \mathrm{M}_\odot$, and a $z = 0$ gravitational softening of 710 pc.

The *IllustrisTNG* simulation that we employ, TNG100, has the same initial conditions (modulo minor differences in the cosmology) and resolution as *Illustris-1*, but improvements to the numerical method and an updated physical model intended to alleviate many of the discrepancies between the *Illustris* results and observations are employed. We note that the aforementioned discrepancies refer to the overall galaxy population, such as the $z = 0$ galaxy colour bimodality; the properties of SMGs, which represent an 'extreme' sub-population of galaxies, were not considered. The updated numerical method and physical model are described in Pillepich et al. (2018a) and Weinberger et al. (2017), and further details about the simulations and first results are presented in various works (e.g. Springel et al. 2018; Pillepich et al. 2018b; Nelson et al. 2018; Naiman et al. 2018). The *IllustrisTNG* model was tuned to reproduce the SFR density as a function of redshift and $z = 0$ galaxy stellar mass and stellar mass–halo mass relations, and the BH mass–stellar mass relation, halo gas fractions and stellar half-mass radii of galaxies were also considered; see section 3.2 of Pillepich et al. (2018a). We refer the interested reader to those works for full details, and we will only highlight the modifications most relevant to the present work here. Regarding the AGN feedback model, the low-accretion state mode was changed to a kinetic model (Weinberger et al. 2017). When computing the Bondi-Hoyle accretion rate, a boost factor is no longer employed; to prevent too-slow early BH growth, a larger seed mass ($8 \times 10^5 h^{-1}\ \mathrm{M}_\odot$, rather than the value of $10^{-5} h^{-1}\ \mathrm{M}_\odot$ used in *Illustris*) is assumed. A few aspects of the model for stellar feedback-driven winds were also changed (Pillepich et al. 2018a). First, the wind calls are kicked isotropically rather than in a bipolar manner. A redshift dependence and floor for the wind velocity are also employed. Also, unlike in *Illustris*, a fraction of the wind energy is deposited as thermal (rather than kinetic) energy (Marinacci et al. 2014), and a metallicity dependence of the mass loading factor, such that winds are less effective at higher metallicity, is assumed.

2.2 Generating simulated SMG catalogues

As discussed in Section 1, to identify SMGs in the simulation, it is ideal to compute individual simulated galaxies' submm flux densities via dust radiative transfer. The mass and spatial resolution of *Illustris* and *IllustrisTNG* are insufficient to resolve the sub-kpc structure of the ISM, and owing to both the sub-grid equation of state treatment of stellar feedback and resolution, such simulations tend to feature overly puffy discs and thus underestimate the attenuation (Trayford et al. 2017). Consequently, we do not perform radiative transfer directly. Instead, we use the following relation based on the results of performing radiative transfer on higher-resolution hydrodynamical simulations of idealised isolated discs and mergers (Hayward et al. 2011, 2013a):

$$\frac{S_{850}}{[\mathrm{mJy}]} = 0.81 \left(\frac{\mathrm{SFR}}{100\ [\mathrm{M}_\odot\ \mathrm{yr}^{-1}]} \right)^{0.43} \left(\frac{M_{\mathrm{dust}}}{10^8\ [\mathrm{M}_\odot]} \right)^{0.54}, \tag{1}$$

where SFR is the 'instantaneous' SFR associated with the star-forming gas cells (for consistency with Hayward et al. 2011) and M_{dust} is the dust mass. When applying the relation, following Hayward et al. (2013b), we incorporate a scatter of 0.13 dex (independent of SFR and dust mass) assuming a Gaussian distribution (Hayward et al. 2011). The submm flux densities predicted using this relation also agree well with the results of performing dust radiative transfer directly on cosmological zoom simulations (Liang et al. 2018; Cochrane et al. 2019) and a semi-analytic model (A. Benson, private communication). Moreover, by combining the above with the observed SFR-$M_\star$ and $M_{\mathrm{dust}}(M_\star, z)$ relations, one can derive an $S_{850} - M_\star$ relation (Hayward et al. 2013a; Hayward 2012) that agrees reasonably well with that observed for SMGs (Davies et al. 2013). Although given sufficient resolution and unlimited computing time, it would be preferred to perform radiative transfer directly, our approach has the advantage of trivial computational expense, and it may actually be more accurate than direct radiative transfer given the resolution of state-of-the-art large-volume simulations such as *Illustris* and *IllustrisTNG*.

In the above, we approximate the total SFR and ISM metal mass of a simulated galaxy by summing over the values for all cells within 25 kpc of the subhalo centre, excluding those that are contained in subhaloes of the halo under consideration (i.e. those in satellite galaxies; recall that we will compare with observations of resolved SMGs, in which satellite galaxies should typically not be blended with central galaxies). We have confirmed that the results are insensitive to the radial cut employed as long as it is $\gtrsim 10$ kpc. Since dust is likely destroyed in hot halo gas (e.g. McKinnon et al. 2016, 2017; Popping et al. 2017), when computing the ISM metal mass, we only consider 'ISM gas' defined using the temperature-density cut from Torrey et al. (2012):

$$\log_{10}\left(\frac{T}{[K]}\right) < 6 + 0.25 \log_{10}\left(\frac{\rho}{10^{10}\ [\mathrm{M}_\odot\ h^2\ \mathrm{kpc}^{-3}]}\right). \tag{2}$$

Given this value, we then compute the dust mass using a dust-to-metal ratio of 0.4 (Dwek 1998; James et al. 2002). The results are not strongly dependent on the exact dust-to-metal ratio used because of the sub-linear scaling between submm flux density and dust mass (e.g. using a value of 0.5 would boost the submm flux density by ~ 13 per cent).

2.3 Number counts

The process described in the previous subsection yields a submm (850-μm) flux density, S_{850}, for each subhalo in the simulation (in addition to other important properties of each subhalo, including the SFR; stellar, gas, metal, and dust masses; and redshift). Given the SMG catalogues derived from each time snapshot of the simulations, we then compute the number counts and redshift distribution. To determine the cumulative number counts of galaxies, $dN(>S_{850})/d\Omega$, we first calculate the number of sources with a given submm flux per unit comoving volume for each snapshot. Next, we multiply the

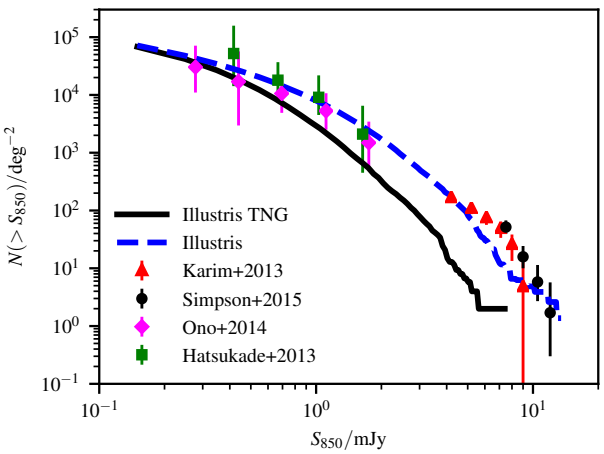

Figure 1. Cumulative 850-μm number counts of SMGs predicted using *IllustrisTNG* (*solid black line*) and *Illustris* (*dashed blue line*). Because we predict the counts of individual SMGs rather than submm source counts for some fixed resolution (i.e. we do not treat blending), we compare only with number counts derived from ALMA observations: Karim et al. (2013, *red triangles*), Simpson et al. (2015, *black circles*), Hatsukade et al. (2013, *green squares*), and Ono et al. (2014, *magenta diamonds*). The *IllustrisTNG* counts are significantly lower than those observed: for $S_{850} \gtrsim 4$ mJy, the counts are under-predicted by 1 dex or more. The *Illustris*-based counts are in excellent agreement with the observed counts at $S_{850} \lesssim 5$ mJy and $S_{850} \gtrsim 9$ mJy, and they are only a factor of ~ 2 lower at intermediate flux densities.

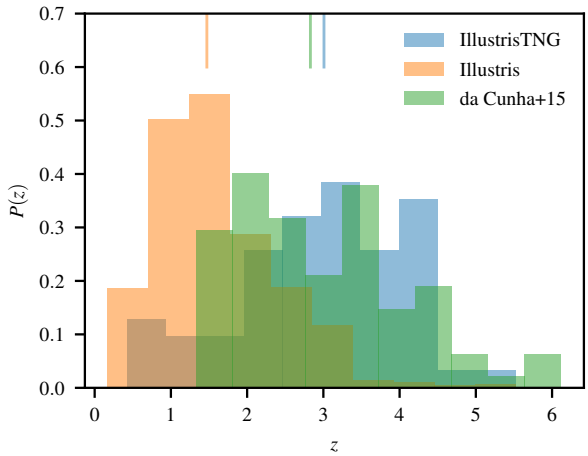

Figure 2. Normalised redshift distributions for the simulated SMGs with $S_{850} \geq 3$ mJy and the observed SMGs from da Cunha et al. (2015). The median values are shown by the vertical bars at the top of the plot. The *IllustrisTNG* redshift distribution is similar to that of the observed sample, whereas the distribution for *Illustris* peaks at significantly lower redshift than observed ($z \sim 1.5$ for *Illustris* vs. $z \sim 2.8$ for the da Cunha et al. 2015 sample).

number density at a given redshift by the redshift-dependent comoving volume element and integrate over redshift (see equation 3 in Hayward et al. 2013a).

3 RESULTS

Fig. 1 compares the 850-μm number counts predicted using *IllustrisTNG* and *Illustris* with those observed. As explained in Section 1, we do not treat the effects of blending due to the coarse angular resolution of single-dish submm telescopes, so we only compare with counts based on interferometric observations with ALMA since such observations have sufficient angular resolution to resolve multi-component sources into individual SMGs (e.g. Karim et al. 2013). The *IllustrisTNG* counts are significantly lower than observed: at $S_{850} \gtrsim 4$ mJy, the observed counts are an order of magnitude or more higher. There are no SMGs in *IllustrisTNG* with $S_{850} \gtrsim 8$ mJy. The counts predicted using *Illustris* are in better agreement with those observed: they are consistent at $S_{850} \lesssim 5$ mJy and $S_{850} \gtrsim 9$ mJy, and they are only a factor of ~ 2 lower than observed at intermediate flux densities.

Fig. 2 compares the redshift distributions of SMGs with $S_{850} > 3$ mJy in the two simulations with the observed distribution for the ALESS sample (da Cunha et al. 2015). In contrast with the number counts, for the redshift distribution, *IllustrisTNG* is in much better agreement with observations. The *IllustrisTNG* and observed redshift distributions are broadly consistent, with similar median redshifts (3.0 vs. 2.8). The *Illustris* redshift distribution peaks at a much lower redshift, 1.5, and differs dramatically from that observed. It is interesting that *IllustrisTNG* matches the observed redshift distribution significantly better than *Illustris*, but given that *IllustrisTNG* under-predicts the number counts by more than an order of magnitude, it is unclear whether this agreement is meaningful or purely coincidental.

To understand the underlying reason(s) for the discrepancies between the counts predicted using *IllustrisTNG* and *Illustris*, in Fig. 3, we show the distribution of the mock SMGs in the SFR-M_{dust} plane (blue circles) for *IllustrisTNG* (top panel) and *Illustris* (bottom panel). Only simulated galaxies with $S_{850} > 3$ mJy are plotted. The dashed lines show contours for various S_{850} values assuming $z = 2$; recall that in our model, the simulated galaxies' SFRs, dust masses, and redshifts fully determine their submm flux densities (see Eq. 1).[1] The other points represent observed SMGs from da Cunha et al. (2015) and Miettinen et al. (2017).[2] The SFR and M_{dust} values for the observed SMGs were obtained by fitting their UV–mm spectral energy distributions (SEDs) with the MAGPHYS SED modelling code, which has been demonstrated to be able to accurately recover these and other galaxy properties by applying the code to simulated galaxy SEDs, for which the 'ground truth' is known (Michałowski et al. 2012; Hayward & Smith 2015; Smith & Hayward 2015, 2018). Because we plot the simulated SMGs taken from all redshift snapshots rather than the results for a lightcone covering an area equal to that probed by the observations, the densities of the simulated and observed points in a given region should not be directly compared, but the plots are useful for determining whether the simulations and observations span the same range of SFR and M_{dust} values. Moreover, because *Illustris* and *IllustrisTNG* have identical volumes (and initial conditions modulo minor differences in the cosmology), directly comparing the density of points for the simulations in the two panels is meaningful.

The most significant difference between *IllustrisTNG* and *Illustris*

[1] Because we include scatter when computing S_{850} using Eq. (1), many of the simulated SMGs with assigned $S_{850} > 3$ mJy lie on the lower-flux side of the $S_{850} = 3$ mJy contour.

[2] One SMG from Miettinen et al. (2017) with SFR $= 6501\,\mathrm{M}_{\odot}\,\mathrm{yr}^{-1}$ and $M_{\mathrm{dust}} = 1.7 \times 10^{8}\,\mathrm{M}_{\odot}$ has been omitted to avoid excess white space.

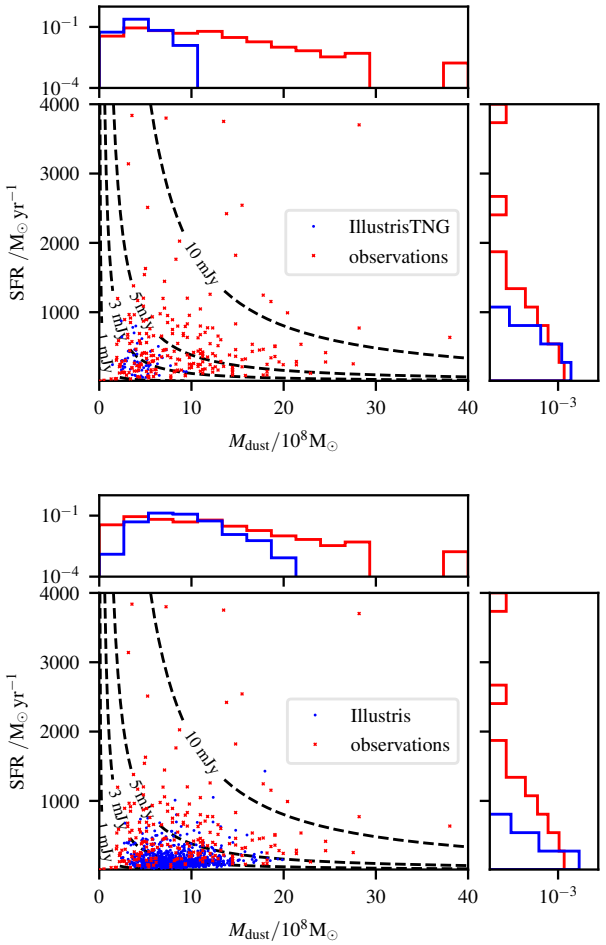

Figure 3. Distribution of simulated SMGs with $S_{850} > 3$ mJy in the SFR–$M_{\rm dust}$ plane (*blue circles*) for *IllustrisTNG* (*top panel*) and *Illustris* (*bottom panel*). The *black dashed lines* are contours of constant submm flux density (S_{850} = 1, 3, 5, and 10 mJy) calculated using Eq. (1) assuming $z = 2$. Observed SMGs from da Cunha et al. (2015) and Miettinen et al. (2017) are shown as *red x's* for comparison. The probability density functions for the simulated and observed SMGs are shown in the marginal plots. The simulated galaxies from *Illustris* span much of the SFR–$M_{\rm dust}$ region occupied by the observed SMGs, whereas both the $M_{\rm dust}$ and, to a lesser extent, SFR values of the *IllustrisTNG* galaxies are significantly lower than those of the observed bright SMGs.

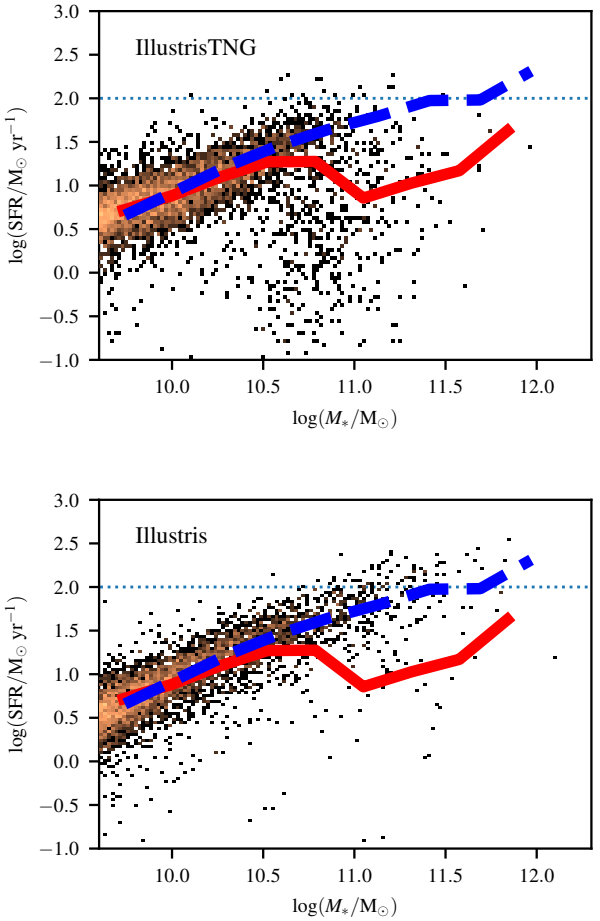

Figure 4. SFR vs. stellar mass for *IllustrisTNG* (*top panel*) and *Illustris* (*bottom*) at $z = 2$. All simulated galaxies with $M_\star \gtrsim 10^{9.5}$ M$_\odot$ are plotted (no SFR cut has been applied). The red solid (blue dashed) lines show the running median SFR for *IllustrisTNG* (*Illustris*). The horizontal lines are intended only to guide the eye. The SFR–$M_\star$ relations of *IllustrisTNG* and *Illustris* are similar for $M_\star \lesssim 10^{10.5}$ M$_\odot$, but at higher masses, the *IllustrisTNG* galaxies have lower SFRs and a greater quenched fraction.

is that simulated galaxies in the former have significantly lower dust masses, with no *IllustrisTNG* galaxies having $M_{\rm dust} \gtrsim 9\times10^8$ M$_\odot$. In contrast, *Illustris* contains many simulated galaxies with dust masses greater this value. For reference, the observed SMGs in the ALESS sample (for which the number counts from Karim et al. 2013 are plotted as red dots in Fig. 1) have a median dust mass of 5.6×10^8M$_\odot$, and the 16th-84th-percentile range of the likelihood distribution is $(0.22 - 11) \times 10^9$M$_\odot$ (da Cunha et al. 2015). Some galaxies in *Illustris* have dust masses that are a factor of two higher than that of the most dust-rich galaxy in *IllustrisTNG*, and as shown below, $z \approx 2$ galaxies with $M_\star \approx 10^{11}$M$_\odot$ (i.e. 'typical SMGs' in the simulations) in *IllustrisTNG* have dust masses that are typically a factor of 3 lower than those of their *Illustris* counterparts. Since in Eq. 1, $S_{850} \propto M_{\rm dust}^{0.54}$, a factor of three higher dust mass corresponds to a $\sim$ 80 per cent higher submm flux density. Given the steepness of the number counts, the relatively modest boost in flux density due to the higher dust masses of the *Illustris* galaxies makes the *Illustris* counts agree much better with observations (Fig. 1).

The *IllustrisTNG* galaxies also exhibit lower SFRs, although the difference in the SFR distributions of *Illustris* and *IllustrisTNG* is less significant than for $M_{\rm dust}$. In *IllustrisTNG*, 16 $z = 2$ galaxies have SFR > 500 M$_\odot$ yr^{-1}, and the maximum SFR reached is 896 M$_\odot$ yr^{-1}. *Illustris* has 29 $z = 2$ galaxies with SFR > 500 M$_\odot$ yr^{-1}, and the most rapidly star-forming galaxy has SFR = 1429 M$_\odot$ yr^{-1}.

In Fig. 3, we only considered simulated galaxies with $S_{850} > 3$ mJy. We will now compare some key properties of all massive galaxies in *Illustris* and *IllustrisTNG*, which will further highlight the reasons for the differences between the *Illustris* and *IllustrisTNG* SMG number counts. We focus on $z \sim 2$ for this analysis because the SMG redshift distribution peaks around that redshift (e.g. Chapman et al. 2005). Fig. 4 shows the distribution of all *IllustrisTNG* (top panel) and *Illustris* (bottom) galaxies in the $z = 2$ snapshot with $M_\star \gtrsim 10^{9.5}$ M$_\odot$ in the SFR–$M_\star$ plane. At $M_\star \lesssim 10^{10.5}$ M$_\odot$, both simulations feature a tight 'star formation main sequence' (SFMS; Noeske et al. 2007;

Daddi et al. 2007; see Sparre et al. 2015 and Donnari et al. 2019 for detailed analyses of the SFR–$M_\star$ relations in *Illustris* and *IllustrisTNG*, respectively), and the typical SFR values at fixed stellar masses are similar. At higher masses, many of the simulated galaxies are 'quenched' (i.e. lie significantly below the main sequence), with a greater fraction of quenched galaxies in *IllustrisTNG* than in *Illustris*; how the quenched fractions in the simulations compare with observational constraints will be discussed in Section 4. Moreover, the typical SFRs are somewhat less in *IllustrisTNG* than in *Illustris*: at $z = 2$ and $M_\star \sim 10^{11}\,\mathrm{M}_\odot$ (a representative stellar mass for bright SMGs), the median SFR in *IllustrisTNG* is $7\,\mathrm{M}_\odot\,\mathrm{yr}^{-1}$, whereas the corresponding value for *Illustris* is $63\,\mathrm{M}_\odot\,\mathrm{yr}^{-1}$. This difference is partially due to *IllustrisTNG* having a lower normalisation for the $z \sim 2$ SFMS (Donnari et al. 2019) (and consequently a lower cosmic SFR density at 'cosmic noon'; see fig. 4 of Pillepich et al. 2018a) compared to *Illustris* and partly because of the higher quenched fraction in this mass and redshift range in *IllustrisTNG*. This indicates that one or more of the differences between the *Illustris* and *IllustrisTNG* galaxy formation models results in systematically lower star formation rates for massive $z \sim 2$ galaxies – and consequently less SMGs – in *IllustrisTNG* compared with *Illustris*.

From Fig. 3, we saw that galaxies in *IllustrisTNG* tend to have lower dust masses than those in *Illustris*. Recall that in our model, the dust masses of the simulated galaxies are determined by their ISM cold gas-phase metal masses, so the differences in the $M_{\rm dust}$ values must be driven by differences in gas masses or/and metallicities. Fig. 5 shows dust mass (first row), gas mass (second row), and metallicity (third row) vs. stellar mass for *IllustrisTNG* (left column) and *Illustris* (right column); all $z = 2$ galaxies with $M_\star \gtrsim 10^{9.5}\,\mathrm{M}_\odot$ are plotted. The first row of Fig. 5 shows that at $z = 2$ and $M_\star \gtrsim 10^{9.5}\,\mathrm{M}_\odot$, the *IllustrisTNG* galaxies have systematically lower dust masses (at fixed stellar mass) than the *Illustris* galaxies, and the difference is greater (a factor of a few) at $M_\star \gtrsim 10^{10.5}\,\mathrm{M}_\odot$. At $z = 2$ and $M_\star \sim 10^{11}\,\mathrm{M}_\odot$, the median $M_{\rm dust}$ values in *IllustrisTNG* and *Illustris* are 7.6×10^7 and $4.2 \times 10^8\,\mathrm{M}_\odot$, respectively, a factor of 3 difference. The second row shows that this discrepancy is primarily due to the *IllustrisTNG* galaxies having lower gas masses than the *Illustris* galaxies at fixed stellar mass: at $z = 2$ and $M_\star \sim 10^{11}\,\mathrm{M}_\odot$, the ISM gas masses are a factor of ~ 2 lower in *IllustrisTNG* than in *Illustris*; the median values are 1.9×10^{10} and $5.5 \times 10^{10}\,\mathrm{M}_\odot$, respectively. The normalisation of the $z = 2$ mass–metallicity relation at $M_\star \gtrsim 10^{10.5}\,\mathrm{M}_\odot$ is also lower in *IllustrisTNG* than in *Illustris* (third row), but the magnitude of this discrepancy is much less than for the gas mass. Again for $z = 2$ and $M_\star \sim 10^{11}\mathrm{M}_\odot$, the median $Z/\mathrm{Z}_\odot$ values for *IllustrisTNG* and *Illustris* are 0.49 and 0.92, a difference of only ~ 30 per cent. Consequently, the differences in gas mass are primarily responsible for the differences in dust mass between the two simulations.

To further highlight the differences between the simulations that drive the differences in their SMG populations, Fig. 6 shows the distributions of SFR and $M_{\rm dust}$ for galaxies at $z = 2$ with stellar masses of $M_\star \sim 10^{11}\mathrm{M}_\odot$ ($10.8 < \log(M_\star/\mathrm{M}_\odot) < 11.2$). Both the SFR (top panel) and dust mass (bottom panel) distributions of the $z = 2$ $M_\star \sim 10^{11}\mathrm{M}_\odot$ galaxies in *IllustrisTNG* are systematically offset to lower values relative to those for *Illustris* galaxies. Even at this high stellar mass, the SMG selection tends to select only galaxies in the high-SFR or/and high-$M_{\rm dust}$ tails of the distributions (e.g. in our model, a $z = 2$ galaxy with SFR $= 100\,\mathrm{M}_\odot\,\mathrm{yr}^{-1}$ and $M_{\rm dust} = 10^{8.5}\,\mathrm{M}_\odot$ has $S_{850} = 1.5$ mJy). Consequently, it is clear that the relative lack of SMGs in *IllustrisTNG* compared to *Illustris* occurs because there are significantly fewer galaxies in both the high-SFR and high-$M_{\rm dust}$ tails of the distributions in *IllustrisTNG*.

Given that it would be prohibitively computationally expensive to run many variants of the simulations considered here, systematically varying the sub-grid feedback models one-by-one, solely for the purpose of the present work, it is somewhat challenging to identify which change(s) to the feedback models cause *IllustrisTNG* to host significantly fewer SMGs than *Illustris*. However, since the simulations use identical initial conditions, it is instructive to consider how the properties of matched individual galaxies differ between the two simulations. For a given halo hosting an SMG with $S_{850} > 2$ mJy in *IllustrisTNG* at a given redshift, we search *Illustris* for the halo at the same redshift whose center is closest to that of the *IllustrisTNG* halo and confirm that the two halos' virial masses differ by less than 30 per cent; we do the same for the halos that host SMGs in *Illustris*. Fig. 7 presents this comparison for the SFR–$M_{\rm dust}$ plane for SMGs in the $z = 2$ snapshot of *IllustrisTNG* (top panel) and *Illustris* (bottom panel). The top panel shows the positions of the *IllustrisTNG* SMGs in the SFR–$M_{\rm dust}$ plane as black points. Each of these galaxies is connected to the matched *Illustris* halo (blue points) by a line. The plot reveals that for all of the 6 $z = 2$ SMGs in *IllustrisTNG*, the corresponding galaxy in *Illustris* has similarly high SFR and $M_{\rm dust}$ mass values. For individual galaxies, the median ratio of the stellar mass (not shown) in *Illustris* to that in *IllustrisTNG* is 0.94. The median SFR ratio is 0.81, and the median dust mass ratio is 1.1. Consequently, halos that host SMGs in *IllustrisTNG* tend to host galaxies with similarly high submm flux densities in *Illustris*.

The bottom panel of Fig. 7 shows a similar comparison but for the 79 $z = 2$ SMGs in *Illustris*. In contrast with the top panel, this plot indicates that most of these galaxies have significantly lower SFR or/and $M_{\rm dust}$ values in *IllustrisTNG*. The median ratio of individual *Illustris* SMGs' stellar masses (not shown) in *IllustrisTNG* to the corresponding value for *Illustris* is 0.76. The median ratios for the SFR, dust mass, and gas mass (not shown) are 0.12, 0.17, and 0.24, respectively, indicating that halos that host SMGs in *Illustris* typically host galaxies with order-of-magnitude-lower SFRs and dust masses in *IllustrisTNG*. Taken together, these plots demonstrate that some change(s) to the feedback model in *IllustrisTNG* relative to the *Illustris* model have caused most of the SMGs in *Illustris* to 'drop out' of the SMG population in *IllustrisTNG*, primarily by decreasing the gas mass and thus both SFR and dust mass. One of the primary drivers of the changes to the sub-grid models in *IllustrisTNG* relative to those in *Illustris* was the need to quench galaxies more effectively. Although this goal has been achieved in *IllustrisTNG* in the sense that a $z = 0$ colour bimodality consistent with observations is obtained, it seems that the highest-mass galaxies are now being quenched slightly too early, causing the SMG counts to be under-predicted by *IllustrisTNG*.

4 DISCUSSION

4.1 SMGs as a constraint on galaxy formation models

We have shown that the SMG number counts predicted using *IllustrisTNG* are significantly lower than observed, whereas those predicted using *Illustris* agree better with observations; the reasons for this difference are that massive ($M_\star \sim 10^{11}\mathrm{M}_\odot$) $z \sim 2$ galaxies in *IllustrisTNG* tend to have significantly lower SFRs and dust masses (primarily due to having lower gas masses) than in *Illustris*. This difference holds not only statistically but also for matched halos in the two simulations. We conclude that one or more of the differences between the sub-grid feedback models employed in *Illustris* and *IllustrisTNG* – likely those for stellar feedback-driven outflows or/and AGN feedback – are responsible for these differences.

Overall, *IllustrisTNG* is more successful than *Illustris* at matching

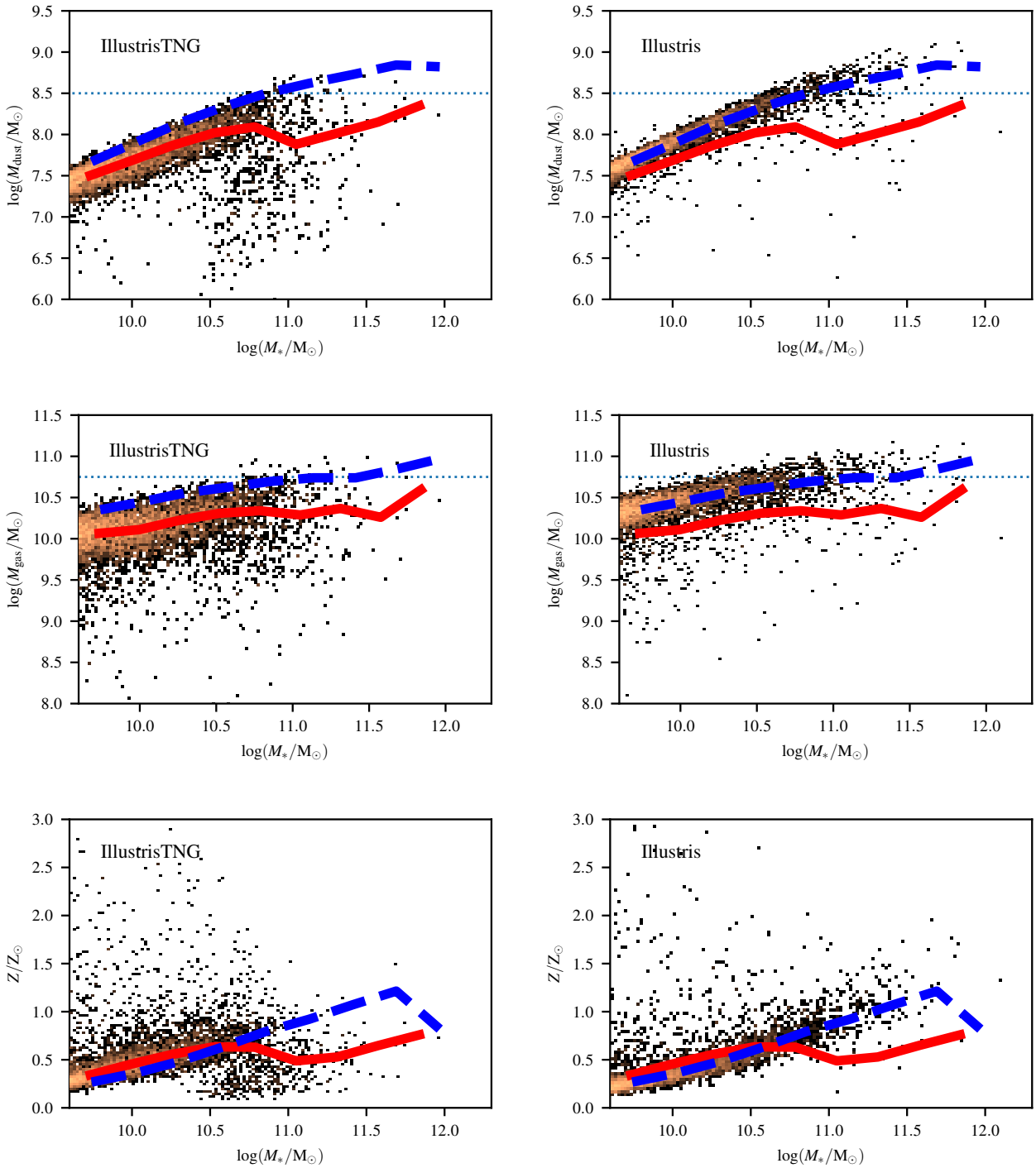

Figure 5. Dust mass (*first row*), gas mass (*second row*), and metallicity (*third row*) vs. stellar mass at $z = 2$ for *IllustrisTNG* (*left column*) and *Illustris* (*right column*). The red solid (blue dashed) lines indicate the running medians for *IllustrisTNG* (*Illustris*). The horizontal lines are intended only to guide the eye. The *IllustrisTNG* galaxies have systematically lower dust masses than those in *Illustris*, especially at high stellar masses ($M_\star \gtrsim 10^{10.5}\,{\rm M}_\odot$). This difference is primarily driven by the *IllustrisTNG* galaxies having lower gas masses at fixed stellar mass. The normalisation of the $z = 2$ mass–metallicity relation at $M_\star \gtrsim 10^{10.5}\,{\rm M}_\odot$ is also slightly lower in *IllustrisTNG* than in *Illustris*, but in terms of the effects on dust masses, the metallicity differences are subdominant to the differences in gas masses.

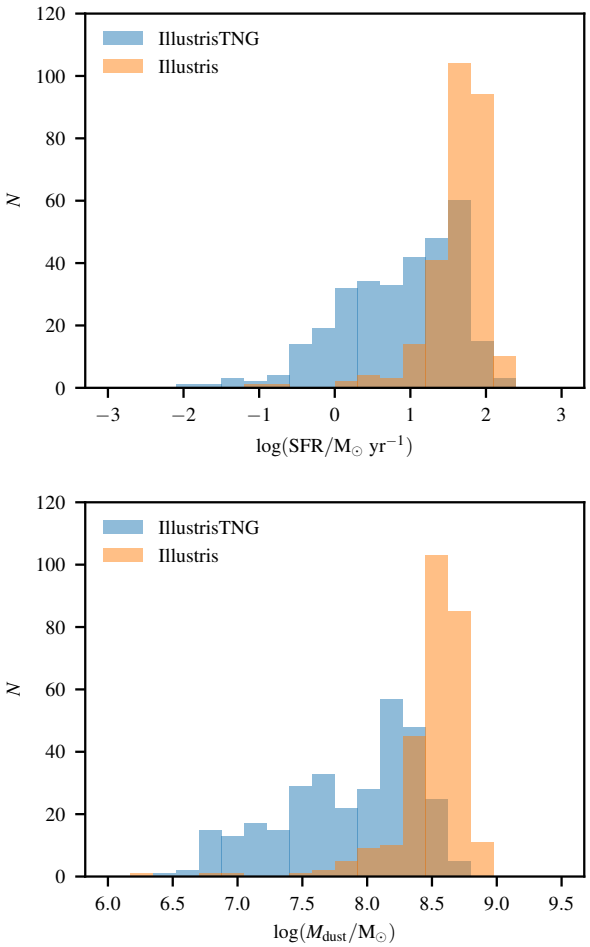

Figure 6. SFR (*top*) and dust mass (*bottom*) for galaxies at $z = 2$ with $10.8 < \log(M_\star/\mathrm{M}_\odot) < 11.2$ in *Illustris* (*blue*; $N = 274$) and *IllustrisTNG* (*orange*; $N = 312$). For both SFR and dust mass, the *Illustris* distributions are offset to higher values relative to the *IllustrisTNG* distributions. SMGs tend to correspond to galaxies in the high-SFR and high-$M_{\rm dust}$ tails of the distributions. Consequently, the fact that the highest SFR and $M_{\rm dust}$ bins are significantly less populated in *IllustrisTNG* than in *Illustris* causes the former to host many fewer SMGs.

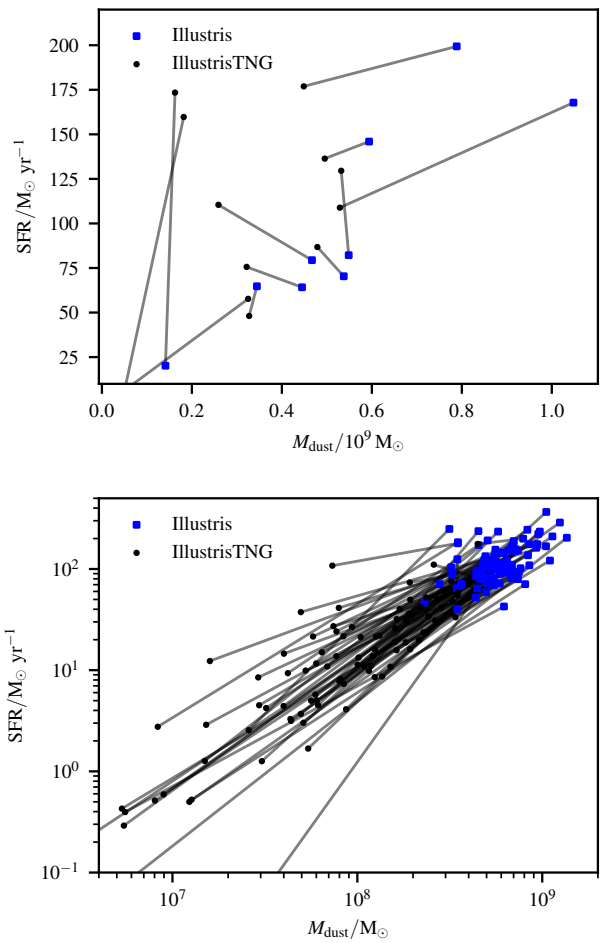

Figure 7. *Top:* The positions of the 11 $z = 2$ SMGs with $S_{850} > 2$ mJy in *IllustrisTNG* (blue points) in the SFR–$M_{\rm dust}$ plane and the corresponding galaxies in *Illustris* (black points; lines connect points corresponding to the same halo in different simulations). *Bottom:* Similar, but for the 79 $z = 2$ SMGs with $S_{850} > 2$ mJy in *Illustris*. The top panel shows that the halos that host SMGs in *IllustrisTNG* host massive galaxies with similar SFR and $M_{\rm dust}$ (and thus S_{850}) values in *Illustris*; in contrast, the bottom panel shows that most of the galaxies that are SMGs in *Illustris* have drastically reduced SFRs or/and dust masses in *IllustrisTNG*, indicating that the differences in the feedback models cause most of the *Illustris* SMGs to 'drop out' of the *IllustrisTNG* SMG population.

various more-general observational constraints. In particular, multiple lines of evidence indicated that the quenching of star formation in *Illustris* was too inefficient (see Nelson et al. 2015 for a detailed discussion), and the changes to the sub-grid feedback models were partially motivated by the need to rectify this issue (Weinberger et al. 2017, 2018; Nelson et al. 2018). The models employed in *IllustrisTNG* result in more-efficient quenching, yielding a $z = 0$ bimodal colour distribution consistent with that observed. However, the resulting galaxy morphology–colour and morphology–size relations are inconsistent with observations, suggesting that further refinement of the quenching model is necessary (Rodriguez-Gomez et al. 2019). Our results provide additional support for this, suggesting that massive $z \sim 2$ galaxies are too efficiently quenched in *IllustrisTNG* (but see Donnari et al. 2019 for a comparison of the quenched fractions at $z \sim 1.75$ in *Illustris* and *IllustrisTNG* with observational constraints). This may indicate that the *timing* of quenching of massive galaxies is still not correct; we discuss this issue in more detail in the next subsection.

Our results reinforce the need to satisfy multiple observational constraints, such as the stellar mass function at different redshifts, before a model for the SMG population can be considered successful. In their hybrid 'semi-empirical' model, which obtained good agreement with observed SMG number counts, Hayward et al. (2013a) partially avoided the issues encountered here by matching the stellar mass functions and gas fractions of massive $z \sim 2$ galaxies *by construction*; the 'added value' was provided by including the effects of mergers based on hydrodynamical simulations and performing radiative transfer to self-consistently compute submm fluxes. In contrast, models that have attempted to self-consistently reproduce the SMG population in an 'ab initio' manner have generally come up short because they do not reproduce the observed counts or other properties of SMGs, they employ simplifications that are unlikely to be valid in

detail, or they incorporate IMF variations that are not well-motivated by theory or observations.

For example, in the large-volume simulation of Davé et al. (2010), the 'SMGs' (selected assuming a monotonic mapping between SFR and submm flux, which should not hold in detail due to the influence of dust mass on the SED shape) have SFRs a factor of ~ 3 less than observed. Also using a large-volume cosmological simulation, Shimizu et al. (2012) predicted SMG number counts in reasonable agreement with those observed, but, as discussed above, their simple model for computing the submm flux likely causes them to over-predict the submm flux and thus counts compared with more accurate calculations. Based on a single cosmological zoom simulation, Narayanan et al. (2015) claimed that 'typical' massive galaxies undergo a long-lived SMG phase and suggested that their model would predict counts consistent with those observed. However, the central galaxy in their simulation is a bright SMG ($S_{850} > 5$ mJy) only once the dust mass exceeds $\sim 5 \times 10^9 \mathrm{M}_\odot$; this value is greater than the dust masses inferred via SED modelling for any of the ALMA-resolved SMGs from da Cunha et al. (2015) and Miettinen et al. (2017). Note that their simulation did not include AGN feedback, which is believed to be a crucial ingredient to match other observational constraints, and our work suggests that the treatment of AGN feedback can significantly affect the predictions for the SMG population (see also Lacey et al. 2016). Moreover, subsequent works employing an improved version of the stellar feedback model used in Narayanan et al. (2015) have found that massive galaxies are insufficiently quenched (Su et al. 2019, 2020). The lack of AGN feedback may explain why Narayanan et al. (2015) obtained such high dust masses (up to $\sim 8 \times 10^9 \mathrm{M}_\odot$ for the central galaxy at the end of the simulation, $z = 2$). The semi-analytic models that are able to match SMG number counts either employ top-heavy IMFs (Baugh et al. 2005; Lacey et al. 2016) or 'non-traditional' scalings for stellar feedback-driven outflows (Safarzadeh et al. 2017), and it remains unclear whether these assumptions are consistent with other observational constraints and physical arguments.

Given the above, we conclude that producing SMGs in sufficient number with properties consistent with those observed remains a challenge for theorists, and further work, both observational and theoretical, regarding this population is sorely needed. Because reproducing the SMG population in a cosmological context is so difficult, they are useful for constraining sub-grid feedback models employed in cosmological simulations. With the exception of the GALFORM SAM, SMGs are typically not considered when tuning existing sub-grid models or building new ones, perhaps because of the perceived complexity of predicting SMG number counts (assuming that radiative transfer calculations are required). However, this can change. The simple method for predicting submm flux that we have employed enables predicting SMG number counts from large-volume cosmological simulations with negligible additional computational expense. Consequently, the observed SMG number counts and redshift distribution can be used as additional constraints on feedback models that are sensitive to regions of the galaxy parameter space (namely, high mass, SFR, and redshift) that traditional comparisons tend not to probe. The utility of SMGs for constraining galaxy formation physics will continue to increase as the community observes larger samples of submm sources with ALMA to more accurately determine the number counts, especially at high flux densities and at high redshift. One particularly interesting application will be constraining variations in the IMF (as has been the case for more than a decade): if the next generation of large-volume simulations is able to reproduce many properties of the population of less extreme galaxies even better than is currently the case but still cannot reproduce the SMG number counts and redshift distribution, this may indeed be (indirect) evidence for IMF variation in SMGs.

4.2 Quenched galaxies at $z \sim 2-3$ and their relationship to SMGs

As discussed above, our results suggest that massive ($M_\star \sim 10^{11} \mathrm{M}_\odot$) $z \sim 2-3$ galaxies are being quenched too early in *IllustrisTNG*. It should thus be instructive to compare the quenched fractions of massive $z \sim 2-3$ galaxies in the simulations with those observed. Donnari et al. (2019) show that the *IllustrisTNG* quenched fraction at this mass at $z \lesssim 1.75$ is consistent with the observations of Muzzin et al. (2013), of order 50 per cent. Moreover, Valentino et al. (2019) find that the number density of quenched galaxies with $M_\star \gtrsim 4 \times 10^{10} \mathrm{M}_\odot$ at $z \sim 3.5$ predicted by *IllustrisTNG* is broadly consistent with observational constraints (which, however, are uncertain at the order-of-magnitude level). Valentino et al. (2019) also show that the SMG number density at $z \gtrsim 3$ in *IllustrisTNG* predicted using our model is consistent with that observed. However, neither of the aforementioned studies cover the peak of the observed SMG redshift distribution, and $z \sim 2-3$ is the crucial period during which the massive galaxy population transitions from being dominated by dusty star-forming galaxies to being dominated by quenched galaxies (fig. 2 of Martis et al. 2016). Using a significantly larger sample than previous studies, Sherman et al. (2020) find that *IllustrisTNG* predicts quenched fractions for $M_\star \geq 10^{11} \mathrm{M}_\odot$ galaxies at $1.5 < z < 3$ that are $\sim 2-5$ times greater than observed. If indeed *IllustrisTNG* overpredicts the quenched fraction as suggested by Sherman et al. (2020), we would naturally expect it to underpredict the observed SMG counts.

Given the above results, it is plausible that massive galaxies are being quenched somewhat too early in *IllustrisTNG*. However, the fact that the *IllustrisTNG* redshift distribution agrees well with that observed (see Fig. 2) seems inconsistent with this explanation. Moreover, since it is known that *Illustris* underpredicts the quenched fraction and does not exhibit a $z \sim 0$ colour bimodality consistent with observations, it is unsurprising that the *Illustris* SMG redshift distribution peaks at much lower redshift than observed. Since *IllustrisTNG* underpredicts the submm counts by more than a magnitude, we wish to avoid over-interpreting the agreement in terms of the SMG redshift distribution, but these results clearly demonstrate that both the integral SMG number counts and redshift distribution serve as useful constraints on galaxy formation models.

4.3 Limitations and future work

We will now discuss some limitations and avenues for future work. The simplicity of our model for predicting submm flux densities is an advantage in that it enables predicting SMG number counts from large-volume cosmological simulations with negligible additional computational expense, but its simplicity also brings some limitations. First, the relation tends to over-predict the submm flux densities of fainter (i.e. lower-SFR or/and lower-M_{dust}) SMGs because in such galaxies, the underlying assumption that all of the star formation is obscured can break down. Thus, to apply Eq. 1 to such galaxies, it would be necessary to first estimate the fraction of the SFR that is obscured by dust and then use that value rather than the total SFR (for one possible method to do so, see Popping et al., submitted). Even better would be to perform dust radiative transfer directly on the simulated galaxies if we are convinced that the simulations resolve the clumpy structure of the ISM sufficiently well to make

this meaningful. A useful intermediate step would be to re-derive a scaling relation for submm flux density using higher-resolution, more physical simulations than those originally used (Hayward et al. 2011, 2013a). We have already performed this type of verification on a limited set of simulations (Liang et al. 2018; Cochrane et al. 2019), but more work along these lines would be merited.

Both the simple scaling relations we use and full dust radiative transfer calculations critically depend on the dust mass (specifically the dust mass distribution in the case of the latter). In this work, we employ a cut in temperature-density space to define 'ISM gas' and then multiply the total metal mass in this ISM gas by a constant dust-to-metal ratio in order to approximate the dust mass. Using a 'live' dust model in the simulations (e.g. McKinnon et al. 2016, 2017) would potentially be a more accurate approach, especially since incorporation of dust destruction processes would alleviate the need to identify dust-containing 'ISM gas' with a simple cut like we have done here. Going further, treating the dust as a separate fluid (e.g. Hopkins & Lee 2016; Seligman et al. 2019; McKinnon et al. 2019) may lead to non-negligible differences in the results of radiative transfer calculations (and thus any scaling relation we would derive from them) because e.g. if the dust and gas are not coupled, radiation-pressure-driven outflows may affect the ISM gas and dust differently and may even lead to different grain properties as a function of distance from the galaxy.

Moreover, we found in previous work that *Illustris* (and likely *IllustrisTNG* given that it has the same resolution) has less starbursts (outliers above the SFMS) than observed (Sparre et al. 2015). Sparre et al. (2017) demonstrated that resolution is one cause of the under-prediction of starbursts in *Illustris* by performing cosmological zoom simulations of mergers selected from *Illustris*, keeping the sub-grid model fixed, and finding order-of-magnitude higher SFR enhancements due to mergers in the zooms than in *Illustris*. The fact that *Illustris* matches the observed SMG counts reasonably well suggests that if starbursts were better resolved, the *Illustris* sub-grid model may actually lead to an over-prediction of the SMG counts. Conversely, the SMG counts predicted using the *IllustrisTNG* model may be in better agreement with observations if starbursts are resolved.

5 CONCLUSIONS

We have used a simple scaling relation derived in previous work to predict SMG number counts for the *IllustrisTNG* TNG100 and *Illustris* cosmological hydrodynamical simulations. Our principal conclusions are the following:

(i) The SMG number counts predicted based on *IllustrisTNG* are lower than those observed for $S_{850} \gtrsim 4$ mJy by an order of magnitude or more; in contrast, those based on *Illustris* are in excellent agreement with the observed counts for $S_{850} \lesssim 4$ mJy and $S_{850} \gtrsim 9$ mJy, and they are only a factor of ~ 2 lower than observed for intermediate flux densities. Thus, *Illustris* fares better than *IllustrisTNG* in terms of reproducing the observed SMG population (which mainly corresponds to galaxies with $M_\star \gtrsim 10^{10.5}\,\mathrm{M}_\odot$ at $z \sim 2-4$) despite the latter better satisfying other observational constraints, such as the stellar mass function at $z \lesssim 1$, the $z = 0$ galaxy colour bimodality, the $z \lesssim 2$ massive galaxy quenched fraction, and the gas contents of low-redshift galaxies.

(ii) The redshift distribution of SMGs in *IllustrisTNG* agrees well with that observed, with similar median redshifts (3.0 and 2.8, respectively), whereas that for *Illustris* is biased toward significantly lower redshift than observed (median $z \sim 1.5$).

(iii) The difference between the counts predicted based on the two simulations is due to $z \sim 2$ massive galaxies in *IllustrisTNG* having both lower dust masses (primarily because of lower gas masses rather than lower metallicities) and SFRs at fixed stellar mass compared to *Illustris*.

(iv) In both simulations, SMGs correspond to massive ($M_\star \sim 10^{11}\mathrm{M}_\odot$) galaxies with SFR and dust mass values well above the median value for galaxies at fixed mass and redshift. The high-M_{dust} and, to a lesser extent, high-SFR tails of the distributions are more populated in *Illustris* than in *IllustrisTNG*, which causes the former to host considerably more SMGs.

(v) By comparing the same halos in *Illustris* and *IllustrisTNG*, we find that halos that host SMGs in *IllustrisTNG* tend to host galaxies with similar SFR and M_{dust} values in *Illustris*. However, the converse does not hold: most of the SMG-hosting halos in *Illustris* tend to host galaxies with similar stellar masses but order-of-magnitude or more lower SFR and dust mass values in *IllustrisTNG*.

(vi) Because the *Illustris* and *IllustrisTNG* simulations employ the same initial conditions modulo minor differences in the cosmology, this comparison indicates that the differences in the sub-grid models employed in the two simulations alter the predictions for the SMG population. Overall, our results demonstrate that the SMG population provides important constraints on galaxy formation models.

Our method entails negligible additional computational expense, so in the future, the observed SMG number counts and redshift distribution can be employed as useful 'orthogonal' constraints when developing and tuning the sub-grid feedback models that are necessarily employed in large-volume cosmological simulations, as has been done by some semi-analytic modelling groups for more than a decade.

ACKNOWLEDGEMENTS

We thank Shy Genel, Melanie Habouzit, and Stuart McAlpine for useful discussion. The Flatiron Institute is supported by the Simons Foundation. MS acknowledges support from the European Research Council under ERC-CoG grant CRAGSMAN-646955.

DATA AVAILABILITY

The data underlying this article will be shared on reasonable request to the corresponding author.

References

Barger A. J., Cowie L. L., Sanders D. B., Fulton E., Taniguchi Y., Sato Y., Kawara K., Okuda H., 1998, Nature, 394, 248
Baugh C. M., Lacey C. G., Frenk C. S., Granato G. L., Silva L., Bressan A., Benson A. J., Cole S., 2005, MNRAS, 356, 1191
Blain A. W., Chapman S. C., Smail I., Ivison R., 2004, ApJ, 611, 725
Casey C. M., Narayanan D., Cooray A., 2014, Phys. Rep., 541, 45
Chabrier G., 2003, PASP, 115, 763
Chakrabarti S., Fenner Y., Cox T. J., Hernquist L., Whitney B. A., 2008, ApJ, 688, 972
Chapman S. C., Blain A. W., Smail I., Ivison R. J., 2005, ApJ, 622, 772
Cochrane R. K., et al., 2019, MNRAS, 488, 1779
Cole S., Lacey C. G., Baugh C. M., Frenk C. S., 2000, MNRAS, 319, 168
Cowley W. I., Lacey C. G., Baugh C. M., Cole S., 2015, MNRAS, 446, 1784
Cowley W. I., Lacey C. G., Baugh C. M., Cole S., Frenk C. S., Lagos C. d. P., 2019, MNRAS, 487, 3082
Daddi E., et al., 2007, ApJ, 670, 156

Davé R., Finlator K., Oppenheimer B. D., Fardal M., Katz N., Kereš D., Weinberg D. H., 2010, MNRAS, 404, 1355
Davé R., Anglés-Alcázar D., Narayanan D., Li Q., Rafieferantsoa M. H., Appleby S., 2019, MNRAS, 486, 2827
Davies L. J. M., Bremer M. N., Stanway E. R., Lehnert M. D., 2013, MNRAS, 433, 2588
Donnari M., et al., 2019, MNRAS, 485, 4817
Dunlop J. S., et al., 2017, MNRAS, 466, 861
Dwek E., 1998, ApJ, 501, 643
Eales S., Lilly S., Gear W., Dunne L., Bond J. R., Hammer F., Fèvre O. L., Crampton D., 1999, ApJ, 515, 518
Engel H., et al., 2010, ApJ, 724, 233
Fontanot F., Monaco P., Silva L., Grazian A., 2007, MNRAS, 382, 903
Genel S., et al., 2014, MNRAS, 445, 175
González J. E., Lacey C. G., Baugh C. M., Frenk C. S., 2011, MNRAS, 413, 749
Granato G. L., Lacey C. G., Silva L., Bressan A., Baugh C. M., Cole S., Frenk C. S., 2000, ApJ, 542, 710
Hatsukade B., Ohta K., Seko A., Yabe K., Akiyama M., 2013, ApJ, 769, L27
Hayward C. C., 2012, PhD thesis, Harvard University
Hayward C. C., 2013, MNRAS, 432, L85
Hayward C. C., Hopkins P. F., 2017, MNRAS, 465, 1682
Hayward C. C., Smith D. J. B., 2015, MNRAS, 446, 1512
Hayward C. C., Kereš D., Jonsson P., Narayanan D., Cox T. J., Hernquist L., 2011, ApJ, 743, 159
Hayward C. C., Jonsson P., Kereš D., Magnelli B., Hernquist L., Cox T. J., 2012, MNRAS, 424, 951
Hayward C. C., Narayanan D., Kereš D., Jonsson P., Hopkins P. F., Cox T. J., Hernquist L., 2013a, MNRAS, 428, 2529
Hayward C. C., Behroozi P. S., Somerville R. S., Primack J. R., Moreno J., Wechsler R. H., 2013b, MNRAS, 434, 2572
Hayward C. C., et al., 2018, MNRAS, 476, 2278
Henriques B. M. B., White S. D. M., Thomas P. A., Angulo R. E., Guo Q., Lemson G., Springel V., 2013, MNRAS, 431, 3373
Hickox R. C., et al., 2012, MNRAS, 421, 284
Hodge J. A., et al., 2013, ApJ, 768, 91
Hopkins P. F., Lee H., 2016, MNRAS, 456, 4174
Hughes D. H., et al., 1998, Nature, 394, 241
James A., Dunne L., Eales S., Edmunds M. G., 2002, MNRAS, 335, 753
Karim A., et al., 2013, MNRAS, 432, 2
Kennicutt R. C., 1998, ApJ, 498, 541
Kroupa P., 2001, MNRAS, 322, 231
Lacey C. G., et al., 2016, MNRAS, 462, 3854
Lanz L., Hayward C. C., Zezas A., Smith H. A., Ashby M. L. N., Brassington N., Fazio G. G., Hernquist L., 2014, ApJ, 785, 39
Liang L., Feldmann R., Faucher-Giguère C.-A., Kereš D., Hopkins P. F., Hayward C. C., Quataert E., Scoville N. Z., 2018, MNRAS, 478, L83
Lovell C. C., Geach J. E., Davé R., Narayanan D., Li Q., 2020, arXiv e-prints, p. arXiv:2006.15156
Lu Y., Mo H. J., Weinberg M. D., Katz N., 2011, MNRAS, 416, 1949
Lu Y., et al., 2014, ApJ, 795, 123
Ma J., et al., 2015, ApJ, 812, 88
Marinacci F., Pakmor R., Springel V., 2014, MNRAS, 437, 1750
Marrone D. P., et al., 2018, Nature, 553, 51
Martis N. S., et al., 2016, ApJ, 827, L25
McAlpine S., et al., 2019, MNRAS, 488, 2440
McKinnon R., Torrey P., Vogelsberger M., 2016, MNRAS, 457, 3775
McKinnon R., Torrey P., Vogelsberger M., Hayward C. C., Marinacci F., 2017, MNRAS, 468, 1505
McKinnon R., Kannan R., Vogelsberger M., O'Neil S., Torrey P., Li H., 2019, arXiv e-prints, p. arXiv:1912.02825
Michałowski M. J., et al., 2012, MNRAS, 426, 1845
Michałowski M. J., et al., 2017, MNRAS, 469, 492
Miettinen O., et al., 2017, A&A, 606, A17
Miller T. B., Hayward C. C., Chapman S. C., Behroozi P. S., 2015, MNRAS, 452, 878
Miller T. B., Chapman S. C., Hayward C. C., Behroozi P. S., Bradford M., Willott C. J., Wagg J., 2020, ApJ, 889, 98
Muñoz Arancibia A. M., Navarrete F. P., Padilla N. D., Cora S. A., Gawiser E., Kurczynski P., Ruiz A. N., 2015, MNRAS, 446, 2291
Muratov A. L., Kereš D., Faucher-Giguère C.-A., Hopkins P. F., Quataert E., Murray N., 2015, MNRAS, 454, 2691
Murray N., Quataert E., Thompson T. A., 2005, ApJ, 618, 569
Muzzin A., et al., 2013, ApJ, 777, 18
Naiman J. P., et al., 2018, MNRAS,
Narayanan D., Hayward C. C., Cox T. J., Hernquist L., Jonsson P., Younger J. D., Groves B., 2010, MNRAS, 401, 1613
Narayanan D., et al., 2015, Nature, 525, 496
Nelson D., et al., 2015, Astronomy and Computing, 13, 12
Nelson D., et al., 2018, MNRAS, 475, 624
Noeske K. G., et al., 2007, ApJ, 660, L43
Ono Y., Ouchi M., Kurono Y., Momose R., 2014, ApJ, 795, 5
Pillepich A., et al., 2018a, MNRAS, 473, 4077
Pillepich A., et al., 2018b, MNRAS, 475, 648
Popping G., Somerville R. S., Galametz M., 2017, MNRAS, 471, 3152
Primack J. R., 2012, Annalen der Physik, 524, 535
Rodriguez-Gomez V., et al., 2019, MNRAS, 483, 4140
Safarzadeh M., Hayward C. C., Ferguson H. C., Somerville R. S., 2016, ApJ, 818, 62
Safarzadeh M., Lu Y., Hayward C. C., 2017, MNRAS, 472, 2462
Schaye J., et al., 2015, MNRAS, 446, 521
Schmidt M., 1959, ApJ, 129, 243
Scoville N., 2003, Journal of Korean Astronomical Society, 36, 167
Seligman D., Hopkins P. F., Squire J., 2019, MNRAS, 485, 3991
Sherman S., et al., 2020, MNRAS, 499, 4239
Shimizu I., Yoshida N., Okamoto T., 2012, MNRAS, 427, 2866
Sijacki D., Springel V., Di Matteo T., Hernquist L., 2007, MNRAS, 380, 877
Sijacki D., Vogelsberger M., Genel S., Springel V., Torrey P., Snyder G. F., Nelson D., Hernquist L., 2015, MNRAS, 452, 575
Simpson J. M., et al., 2015, ApJ, 807, 128
Smail I., Ivison R. J., Blain A. W., 1997, ApJ, 490, L5
Smith D. J. B., Hayward C. C., 2015, MNRAS, 453, 1597
Smith D. J. B., Hayward C. C., 2018, MNRAS,
Smith D. J. B., Hayward C. C., Jarvis M. J., Simpson C., 2017, MNRAS, 471, 2453
Somerville R. S., Gilmore R. C., Primack J. R., Domínguez A., 2012, MNRAS, 423, 1992
Sparre M., et al., 2015, MNRAS, 447, 3548
Sparre M., Hayward C. C., Feldmann R., Faucher-Giguère C.-A., Muratov A. L., Kereš D., Hopkins P. F., 2017, MNRAS, 466, 88
Springel V., 2010, MNRAS, 401, 791
Springel V., Hernquist L., 2003, MNRAS, 339, 289
Springel V., Di Matteo T., Hernquist L., 2005, MNRAS, 361, 776
Springel V., et al., 2018, MNRAS, 475, 676
Su K.-Y., et al., 2019, MNRAS, 487, 4393
Su K.-Y., et al., 2020, MNRAS, 491, 1190
Thompson T. A., Quataert E., Murray N., 2005, ApJ, 630, 167
Toft S., et al., 2014, ApJ, 782, 68
Torrey P., Vogelsberger M., Sijacki D., Springel V., Hernquist L., 2012, MNRAS, 427, 2224
Torrey P., Vogelsberger M., Genel S., Sijacki D., Springel V., Hernquist L., 2014, MNRAS, 438, 1985
Trayford J. W., et al., 2017, MNRAS, 470, 771
Valentino F., et al., 2019, arXiv e-prints, p. arXiv:1909.10540
Vogelsberger M., Genel S., Sijacki D., Torrey P., Springel V., Hernquist L., 2013, MNRAS, 436, 3031
Vogelsberger M., et al., 2014a, MNRAS, 444, 1518
Vogelsberger M., et al., 2014b, Nature, 509, 177
Wang L., Pearson W. J., Cowley W., Trayford J. W., Béthermin M., Gruppioni C., Hurley P., Michałowski M. J., 2019, A&A, 624, A98
Weinberger R., et al., 2017, MNRAS, 465, 3291
Weinberger R., et al., 2018, MNRAS, 479, 4056
Wilkinson A., et al., 2017, MNRAS, 464, 1380
da Cunha E., et al., 2015, ApJ, 806, 110

This paper has been typeset from a TEX/LATEX file prepared by the author.